

旋轉圓盤受脈衝外緣力時之非線性振動
Nonlinear Oscillation of a Spinning Disk Under Space-Fixed Pulsating Edge Loads

計畫編號: NSC 89-2212-E-002-106

執行期限: 89年8月1日至90年7月31日

計畫主持人: 陳振山 jschen@w3.me.ntu.edu.tw

執行機關: 國立台灣大學機械系

摘要

本計畫以多重尺度法分析旋轉圓盤受脈衝外緣力作用時，一對前進與後退波之間的內部共振現象。研究結果發現當前進波頻率為後退波頻率的三倍左右，而且外緣力頻率為後退波頻率的兩倍左右時會有內部共振現象。當阻尼小時，旋轉圓盤的無聊解會以叉子式分歧或霍普式分歧的方式失去穩定性。反之，非無聊解可能會發生鞍點式或霍普式的分歧現象。

關鍵詞: 多重尺度法，旋轉圓盤，內部共振

Abstract

Internal resonance between a pair of forward and backward modes of a spinning disk under space-fixed pulsating edge loads is investigated by means of multiple scale method. It is found that internal resonance can occur only at certain rotation speeds at which the natural frequency of the forward mode is close to three times the natural frequency of the backward mode and the excitation frequency is close to twice the frequency of the backward mode. For light damping case the trivial solution can lose stability via both pitchfork as well as Hopf bifurcations when frequency detuning of the edge load is varied. On the other hand, nontrivial solutions experience both saddle-node and Hopf bifurcations.

Keywords: Multiple scale method, spinning disk, internal resonance

Introduction

The vibration analysis of a spinning disk under space-fixed edge loads attracts attention because of its possible application in such fields as circular saw cutting and grind wheel operation. Carlin and his coworkers' investigation [1] appears to be

the first paper attempting to calculate the natural frequencies of a spinning disk under a concentrated radial edge load. Radcliffe and Mote [2] extended the work of [1] by considering a general concentrated edge load with both radial and tangential components. Chen [3,4] reformulated the problem with emphasis on the effects of relative motion between the disk and the edge load on the stability and natural frequencies of the loaded disk. Recently Chen [5] extended these analyses by considering the parametric resonance of a spinning disk under space-fixed pulsating edge loads.

The plate model employed in [5] ignored the effect of membrane stretching. As a consequence the equation of motion is linear in terms of the transverse deflection and the stiffness term involves a periodic coefficient which is due to the pulsating edge load. This linearized model imposes two limits on the applicability of the parametric resonance theory presented in [5]. First of all, while the linearized model can predict the onset of parametric resonance, it cannot predict the amplitude of steady state vibration after parametric resonance occurs. Secondly, it cannot account for the complicated internal resonance phenomenon which is due to interaction between modes coupled by the nonlinear effect.

In this project we extend our previous work [5] to consider the nonlinear parametric resonance of a spinning disk under space-fixed pulsating edge loads. Membrane stretching effect is taken into account by employing von Karman's plate model. We focus our attention on the internal resonance between a pair of forward and backward traveling waves with the same number of nodal diameters and nodal circles.

Equations of Motion

The dimensionless equations of motion of the spinning disk under space-fixed pulsating edge load can be rewritten as

$$w_{,rr} + 2\Omega w_{,r} + \Omega^2 w_{,rr} + \nabla^4 w + Lw + 2\nu c_f w_{,r} + \nu P_k \cos \mathcal{X} L_k w =$$

$$w_{,rr} (r^{-1} W_{3,r} + r^{-2} W_{3,rr}) + (r^{-1} w_{,r} + r^{-2} w_{,rr}) W_{3,rr} - 2(r^{-1} w_{,r})_{,r} (r^{-1} W_{3,rr})_{,r} \quad (1)$$

$$\nabla^4 W_3 = -\mathcal{V} [w_{,rr} (r^{-1} w_{,r} + r^{-2} w_{,rr}) + 2r^{-3} w_{,r} w_{,rr} - r^{-2} (w_{,r})^2 - r^{-4} (w_{,rr})^2] \quad (2)$$

L_k is the membrane operator associated with the stress field due to the edge load, and L is associated with the axisymmetrical stress field due to the centrifugal force.

Discretization

In this paper we focus on the internal resonance between a pair of forward and backward (m, n) modes excited by the in-plane edge load. We assume that solution $w(r, \theta, t)$ of Eqs.(1) and (2) can be approximated in terms of eigenfunctions $w_{mn}(r, \theta)$ as

$$w(r, \theta, t) = c_{mn}(t) w_{mn} + \bar{c}_{mn}(t) \bar{w}_{mn} \quad (3)$$

After substituting Eq.(3) into Eqs.(1) and (2), and following Galerkin's procedure, we can discretize Eqs.(1) and (2) into

$$\ddot{c}_{mn} + 2i\Omega \dot{c}_{mn} + \nu c_{mn} + 2\nu c_f \dot{c}_{mn} + \nu \bar{c}_{mn} \cos \mathcal{X} + \nu r |c_{mn}|^2 c_{mn} = 0 \quad (4)$$

where

$$\begin{aligned} \nu c_{mn} &= \tilde{S}_{mn} \tilde{S}_{m\bar{n}} \\ \nu &= \int_0^1 \int_0^{2\pi} \left[r \dot{r}_{r(2n)} (R_{mn,r})^2 + \left(\frac{n^2 \dot{r}_{r(2n)}}{r} - n \dot{r}_{r(2n),r} \right) (R_{mn})^2 \right] dr \end{aligned}$$

\tilde{S}_{mn} and $\tilde{S}_{m\bar{n}}$ are the natural frequencies of the backward and the forward modes, respectively.

Multiple Scale Method

We apply the method of multiple scale to analyze the solution of Eq.(4). The method of multiple scale assumes an expansion of the solution in the form

$$c_{mn}(t) = c_{mn}^{(0)}(t, T_1) + \nu c_{mn}^{(1)}(t, T_1) + \mathcal{O}(\nu^2) \quad (5)$$

where $T_1 \equiv \mathcal{V}t$. Substituting (5) into (4) and equating coefficients of like powers of ν yields

$$\mathcal{V}^0: D_0^2 c_{mn}^{(0)} + 2i\Omega D_0 c_{mn}^{(0)} + \nu c_{mn}^{(0)} = 0 \quad (6)$$

$\mathcal{V}^1:$

$$D_0^2 c_{mn}^{(1)} + 2i\Omega D_0 c_{mn}^{(1)} + \nu c_{mn}^{(1)} = -2D_1 D_0 c_{mn}^{(0)} - 2i\Omega D_1 c_{mn}^{(0)} - 2c_f D_0 c_{mn}^{(0)} - r |c_{mn}^{(0)}|^2 c_{mn}^{(0)} - \bar{c}_{mn}^{(0)} \cos \mathcal{X} \quad (7)$$

where $D_0 \equiv \frac{\partial}{\partial t}$, and $D_1 \equiv \frac{\partial}{\partial T_1}$. The general

solution of Eq.(6) can be written in the form

$$c_{mn}^{(0)} = d_1(T_1) e^{i\tilde{S}_{mn} T_0} + d_2(T_1) e^{-i\tilde{S}_{m\bar{n}} T_0} \quad (8)$$

Substituting (8) into the right hand side of (7) we observe that there exist secular terms in three different cases. In the first case when $\tilde{S}_{m\bar{n}}$ is close to $3\tilde{S}_{mn}$ and \mathcal{X} is close to $2\tilde{S}_{mn}$ internal resonance involving both modes will occur. In the second case when $\tilde{S}_{m\bar{n}}$ is close to $3\tilde{S}_{mn}$ and \mathcal{X} is close to $2\tilde{S}_{m\bar{n}}$, only single mode resonance will be induced. In the third case when $\tilde{S}_{m\bar{n}}$ is away from $3\tilde{S}_{mn}$ and \mathcal{X} is close to $2\tilde{S}_{mn}$ or $2\tilde{S}_{m\bar{n}}$, again only single mode resonance is possible. The second and the third cases are the same in essence. No combination resonance of the sum or difference type is possible when only this pair of modes are considered [5]. In the following we focus on the internal resonance case.

Internal Resonance

Internal resonance occurs when $\tilde{S}_{m\bar{n}}$ is close to $3\tilde{S}_{mn}$ and \mathcal{X} is close to $2\tilde{S}_{mn}$. In this case we assume that

$$\mathcal{X} = 2\tilde{S}_{mn} + \nu g_1$$

$$\tilde{S}_{m\bar{n}} = 3\tilde{S}_{mn} + \nu g_2$$

where g_1 and g_2 are two independent detuning parameters. The secular terms of Eq.(7) can be eliminated if

$$2i\tilde{S}_{mn} D_1 d_1 + i2\tilde{S}_{mn} c_f d_1 + r d_1 |d_1|^2 + 2d_2 |d_1|^2 \nu^{-1} \bar{c}_{mn} e^{i\tilde{S}_{m\bar{n}} T_0} + d_2 e^{i(\tilde{S}_{m\bar{n}} - \tilde{S}_{mn}) T_0} \nu = 0 \quad (9)$$

$$2i\tilde{S}_{m\bar{n}} D_1 d_2 + i2\tilde{S}_{m\bar{n}} c_f d_2 - r d_2 (|d_2|^2 + 2|d_1|^2) + \bar{c}_{mn} d_1 e^{i(\tilde{S}_{m\bar{n}} - \tilde{S}_{mn}) T_0} \nu = 0 \quad (10)$$

We express d_1 and d_2 in the forms

$$d_1(T_1) = \frac{1}{2} a_1(T_1) e^{iS_1(T_1)} \quad (11)$$

$$d_2(T_1) = \frac{1}{2} a_2(T_1) e^{iS_2(T_1)} \quad (12)$$

After substituting Eqs.(11) and (12) into Eqs.(9) and (10) we can conclude that the nontrivial steady state solutions of a_1 , S_1 , a_2 , and S_2 must satisfy the following equations,

$$4\check{S}_{mn}g_1a_1 - ra_1(a_1^2 + 2a_2^2) + 2\check{~}(a_1 \cos\mathcal{E}_1 + a_2 \cos\mathcal{E}_2) = 0 \quad (13)$$

$$4c_f\check{S}_{mn}a_1 - \check{~}(a_1 \sin\mathcal{E}_1 + a_2 \sin\mathcal{E}_2) = 0 \quad (14)$$

$$4\check{S}_{mn}(2g_2 - 3g_1)a_2 + ra_2(a_2^2 + 2a_1^2) - 2\check{~}a_1 \cos\mathcal{E}_2 = 0 \quad (15)$$

$$4c_f\check{S}_{mn}a_2 + \check{~}a_1 \sin\mathcal{E}_2 = 0 \quad (16)$$

where

$$\mathcal{E}_1 = g_1 T_1 - 2S_1$$

$$\mathcal{E}_2 = (g_2 - g_1)T_1 - S_1 - S_2$$

Steady State Solutions

Figure 1 shows the amplitudes and phases of the steady state solutions as functions of detuning parameter g_1 for the internal resonance between a pair of (0,3) modes at $\Omega = 3.3$. The parameters used in the calculation are $\nu = 0.01$, $\check{S}_{03} = 9.9$, $\check{S}_{0\bar{3}} = 29.7$, $\check{~} = 100$, $c_f = 0.5$, and $r = 0.4$. The excitation frequency $\chi = 2\check{S}_{03} + \nu g_1$. The solid and dashed curves represent stable and unstable solutions, respectively. The stable trivial solution undergoes a super-critical pitchfork bifurcation at $g_1 = -3.11$ (point A). From point A the nontrivial solution branch is stable and undergoes a saddle-node bifurcation at point H ($g_1 = 0.90$). On the other hand, the unstable trivial solution from point A undergoes a sub-critical pitchfork bifurcation at point B ($g_1 = -0.64$), creating an unstable nontrivial branch BH and a stable trivial branch BC. This stable trivial solution then loses stability via a super-critical Hopf bifurcation at $g_1 = -0.33$ (point C), creating a quasiperiodic solution c_{03} which cannot be shown in Fig.1. The unstable branch CD undergoes a super-critical Hopf bifurcation at point D ($g_1 = 0.33$) and creates a stable

trivial branch DE. The branch DE then undergoes a super-critical bifurcation at point E creating a stable nontrivial branch EG and unstable trivial branch EF. The stable branch EG then loses stability via a super-critical Hopf bifurcation at point G creating a stable quasiperiodic solution (which again cannot be shown in Fig.1) and an unstable periodic solution. The trivial branch EF undergoes a sub-critical pitchfork bifurcation at point F creating an unstable nontrivial branch and a stable trivial branch.

The bifurcation points along the trivial solution path can be verified by observing the eigenvalues λ of the Jacobian matrix in Fig.2. At points A, B, E, and F there exists a zero eigenvalue, which implies a pitchfork bifurcation. On the other hand at points C and D there exist a pair of purely imaginary eigenvalues and the real part loci of the eigenvalues cross the zero line “transversely”, which implies a Hopf bifurcation.

To demonstrate the existence of quasiperiodic solutions predicted by the multiple scale analysis we use Runge-Kutta method to integrate Eq.(21) at $g_1 = -0.32$ (a point slightly to the right of point C in Fig.1) with initial conditions $c_{03} = 0.1$ and $\mathcal{I}_{03} = 0$. Figure 3(a) shows the response history of the real part of c_{03} after a long period of time. Figure 3(b) shows its Poincare map recorded from $t=10000$ to 12000 with the sampling rate equal to the excitation frequency. The sampling points fill up a small strip around a closed curve, which implies the quasiperiodic feature of the response. If the initial condition of c_{03} is changed from 0.1 to 20, the response then settles to the stable branch AH in Fig.1, as shown in Fig.4. The Poincare map in Fig.4(b) records the sampling points from $t=4000$ to 6000.

Conclusions

In this paper we use multiple scale method to study the internal resonance between a pair of forward and backward modes of a spinning disk under space-fixed pulsating edge loads. Linear analysis in [5] predicts that only single mode parametric

resonance can occur when the excitation frequency is twice the natural frequency of the mode of interest. By considering the nonlinear effect resulting from von Karman's plate model, however, internal resonance is predicted in some special cases. It is found that internal resonance can occur when the natural frequency of the forward mode is close to three times the natural frequency of the backward mode and the excitation frequency is close to twice the frequency of the backward mode. In the case when the excitation frequency is close to twice the frequency of the forward mode, on the other hand, only single mode parametric resonance is possible.

References

- [1] Carlin, J.F., Appl, F.C., Bridwell, H.C., and Dubois, R.P., 1975, "Effects of Tensioning on Buckling and Vibration of Circular Saw Blades," *ASME Journal of Engineering for Industry*, Vol. 2, pp.37-48.
- [2] Radcliffe, C. J., and Mote, C.D., Jr., 1977, "Stability of Stationary and Rotating Discs Under Edge Load," *International Journal of Mechanical Sciences*, Vol. 19, pp. 567-574.
- [3] Chen, J.-S., 1994, "Stability Analysis of a Spinning Elastic Disk Under a Stationary Concentrated Edge Load," *ASME Journal of Applied Mechanics*, Vol.61, pp.788-792.
- [4] Chen, J.-S., 1996, "Vibration and Stability of a Spinning Disk Under Stationary Distributed Edge Loads," *ASME Journal of Applied Mechanics*, Vol.63, pp.439-444.
- [5] Chen, J.-S., 1997, "Parametric Resonance of a Spinning Disk Under Space-Fixed Pulsating Edge Loads," *ASME Journal of Applied Mechanics*, Vol.64, pp. 139-143.

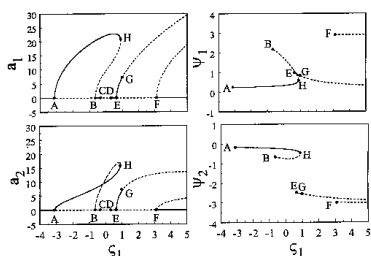


Fig.1

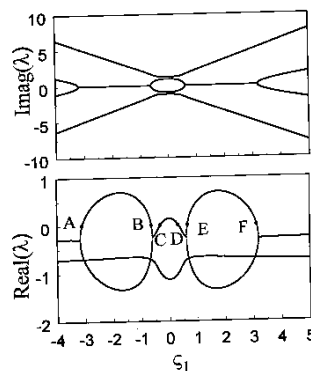


Fig.2

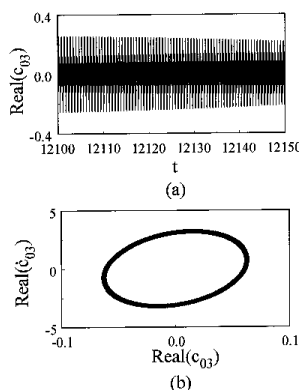


Fig.3

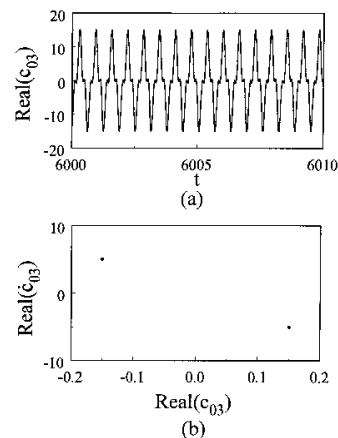


Fig.4

